

**FHS PUBLIC ACCESS**

Author manuscript

Cell Rep. Author manuscript; available in PMC 2017 December 13.

Published in final edited form as:

Cell Rep. 2017 November 21; 21(8): 2313–2325. doi:10.1016/j.celrep.2017.10.093.

## Extensive homeostatic T cell phenotypic variation within the Collaborative Cross

Jessica B. Graham<sup>1</sup>, Jessica L. Swarts<sup>1</sup>, Michael Mooney<sup>2,3</sup>, Gabrielle Choonoo<sup>2,3</sup>, Sophia Jeng<sup>4</sup>, Darla R. Miller<sup>5</sup>, Martin T. Ferris<sup>5</sup>, Shannon McWeeney<sup>2,3,4</sup>, and Jennifer M. Lund<sup>1,6,\*</sup>

<sup>1</sup>Vaccine and Infectious Disease Division, Fred Hutchinson Cancer Research Center, Seattle, WA, 98109, USA

<sup>2</sup>Division of Bioinformatics & Computational Biology, Department of Medical Informatics & Clinical Epidemiology, Oregon Health & Science University, Portland, OR, 97239, USA

<sup>3</sup>OHSU Knight Cancer Center Institute, Oregon Health & Science University, Portland, OR, 97239, USA

<sup>4</sup>Oregon Clinical and Translational Research Institute, Oregon Health & Science University, Portland, OR, 97239, USA

<sup>5</sup>Department of Genetics, University of North Carolina at Chapel Hill, Chapel Hill, NC, 27599, USA

<sup>6</sup>Department of Global Health, University of Washington, Seattle, WA, 98195, USA

### Summary

The Collaborative Cross (CC) is a panel of reproducible recombinant inbred mouse strains with high levels of standing genetic variation, thereby affording unprecedented opportunity to perform experiments in a small animal model containing controlled genetic diversity while allowing for genetic replicates. Here, we advance the utility of this unique mouse resource for immunology research, as it allows for both examination and genetic dissection of mechanisms behind adaptive immune states in mice with distinct and defined genetic makeups. This approach is founded on quantitative trait locus mapping: identifying genetically variant genome regions associated with phenotypic variance in traits-of-interest. Furthermore, the CC can be utilized for mouse model development; distinct strains have unique immunophenotypes and immune properties, making them suitable for research on particular diseases and infections. Here, we describe variation in

\*Corresponding author: Jennifer M. Lund, [jlund@fredhutch.org](mailto:jlund@fredhutch.org).  
Lead Contact: Jennifer M. Lund, [jlund@fredhutch.org](mailto:jlund@fredhutch.org)

#### Author Contributions

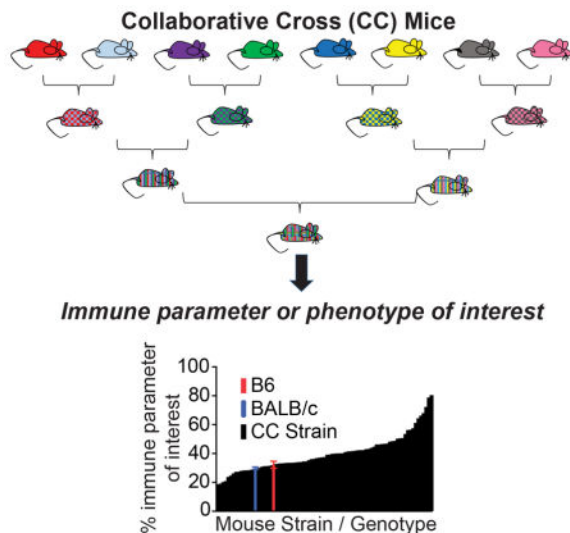
Conceptualization, J.B.G. and J.M.L.; Methodology, J.B.G., M.T.F., and J.M.L.; Formal Analysis, J.B.G., M.M., G.C., S.J., S.M., M.T.F., and J.M.L.; Investigation, J.B.G. and J.S.; Resources, D.R.M., and M.T.F.; Data Curation, J.B.G., M.M., G.C., and S.M.; Writing – Original Draft, J.B.G. and J.M.L.; Writing – Review & Editing, all authors; Visualization, J.B.G. and M.M.; Supervision, J.B.G., S.M., and J.M.L.

**Publisher's Disclaimer:** This is a PDF file of an unedited manuscript that has been accepted for publication. As a service to our customers we are providing this early version of the manuscript. The manuscript will undergo copyediting, typesetting, and review of the resulting proof before it is published in its final citable form. Please note that during the production process errors may be discovered which could affect the content, and all legal disclaimers that apply to the journal pertain.

cellular immune phenotypes across F1 crosses of CC strains, and reveal quantitative trait loci responsible for several immune phenotypes.

## eTOC Blurp

Graham et al. advance the use of the Collaborative Cross (CC), a panel of reproducible recombinant inbred mouse strains, for immunology research. They demonstrate that the CC better models the phenotypic diversity in human T-cell immunity, and use quantitative trait locus mapping to reveal candidate genes linked to T-cell phenotypes.



## Keywords

Adaptive Immunity; Immunogenetics; Mouse Models; Collaborative Cross; QTL Mapping

## Introduction

In seeking to understand the complex interactions and pathways of the human immune response, researchers have long turned to inbred mouse models. 99% of mouse genes are shared with humans (Boguski, 2002), and inbred laboratory mouse strains are well characterized, reproducible, and allow for the use of unique immunological tools such as transgenic or knockout mice. However, given the diverse breadth of clinical outcomes and immune responses observed in the human population, any single traditional inbred mouse model cannot fully capture the range of immune phenotypes expressed across genetically diverse humans. Indeed, while estimates vary, there is a clear contribution of genetic variation in driving diversity throughout human immune responses (Salveti et al., 2000), and this diversity cannot be fully identified through study of a single gene knockout (KO). In order to fully investigate these complex networks, additional studies in a model that better captures the genetic diversity of humans is critical.

Defining the genetic basis of immune responses and regulation requires approaches and model systems that move beyond classical genetic screens, such as targeted KO mouse

strains on a C57BL/6 (B6) background, or random N-ethyl-N-nitrosourea (ENU) mutagenesis studies, which both typically study one gene at a time (Gondo et al., 2010; Mountz et al., 2001; Yates et al., 2009). The Collaborative Cross (CC) mouse genetic reference panel presents a resource which specifically models complex genetic interactions, and therefore expands upon classic approaches within traditional (e.g. B6) mouse models. The CC strains are a recombinant inbred (RI) panel, and are derived from eight founder strains: five classical inbred strains (C57BL/6J, A/J, 129S1/SvImJ, NOD/ShiLtJ, and NZO/SH1LtJ) and three wild-derived strains (CAST/EiJ, PWK/PhJ, and WSB/EiJ). These eight founder strains represent the three major *Mus musculus* subspecies (*domesticus*, *musculus*, and *castaneus*), and capture nearly 90% of common genetic variation in laboratory mouse strains, with this variation uniformly distributed across the genome (Churchill et al., 2004; Threadgill et al., 2011)(Threadgill and Churchill, 2012). CC-RI strains were created by three generations of funnel breeding to incorporate genomic contributions of all eight founder strains within each CC strain, followed by at least 20 generations of inbreeding (Collaborative Cross, 2012). The CC thereby provides a reproducible experimental model of many aspects of genetic variation within the human genome. In these studies, F1 progeny from crosses between CC-RI strains (CC-RIX, recombinant intercross) were used (Graham et al., 2015). These RIX lines were heterozygous for the H-2b<sup>b</sup> major histocompatibility complex (MHC) haplotype, thereby allowing for use of reagents such as tetramers to examine T cell responses in these mice, which is critical to enable study of T cell-mediated immunity.

The CC provides the ability to assess the breadth of phenotypic differences under genetic control, and can also provide new mouse models for human diseases, as screens have identified variations in immune phenotypes and clinical disease symptoms for infections such as influenza (Ferris et al., 2013), Ebola (Rasmussen et al., 2014), West Nile virus (Graham et al., 2016; Graham et al., 2015), SARS (Gralinski et al., 2015), as well as spontaneous colitis (Rogala et al., 2014), cancer-related phenotypes (Reilly, 2016), and behavioral traits (Chesler, 2014). In our studies as part of the Collaborative Cross Systems Immunogenetics Group, we screened over 110 CC-RIX for a variety of immune response parameters at steady-state in adult male mice of 8–10 weeks of age. Importantly, within the screen we found a wide variation in each immune phenotype measured, and here, we fully describe a comprehensive screen of CC-RIX for cell subsets such as CD3<sup>+</sup>, CD4<sup>+</sup>, CD8<sup>+</sup>, and regulatory T cells (Treg), as well as activation markers and inflammatory cytokines. Included with these data are the identity of quantitative trait loci (QTL), or polymorphic host genome regions, and potential candidate genes within these regions which impact immune phenotypes. This initial proof-of-concept genetic mapping as well as our extensive dataset pave the way for future use of CC mice for genetic mapping of immune traits as well as targeted CC mouse strain selection for future immunology and immunogenetics studies. Similar to the expansion of immune phenotypes displayed in the so-called “pet store mice” or “dirty mice” as compared to mice maintained under specific pathogen-free (SPF) conditions, which has allowed for an improved mouse model that better accounts for the microbial colonization diversity in humans (Masopust et al., 2017), we demonstrate here that use of the Collaborative Cross can address another critical limitation of mouse research by

expanding on the genetic diversity and resultant immune phenotypes of murine study subjects to more effectively model human immunity.

## Results

### Screening CC-RIX lines for immune phenotypes

We conducted a comprehensive screen of 113 CC-RIX lines for immune response phenotypes in order to gauge the diversity of responses resulting from natural genetic variation. CC-RIX lines were bred to ensure that lines were heterozygous for the H-2b locus, having one copy of the H-2b<sup>b</sup> haplotype and one copy of the other various haplotypes at the MHC locus. This design was selected such that we could examine antigen-specific T cell responses for our parallel studies of immunogenetics of virus infection, while concurrently maintaining genetic variation throughout the rest of the genome. Through our screen, three to six adult, 8–10 week-old male mice were examined for each CC-RIX line, and we measured and catalogued an extensive list of T cell phenotypes within the spleen at steady-state with no experimental manipulations. The range of phenotypes included frequency of T cell subsets, proportion of cells expressing various activation markers, frequency of cells producing inflammatory cytokines, and quantity of cells expressing tissue migration markers (Supp. Table 1 and Supp. Fig. 1). For each phenotype examined, we measured abundant variability between RIX lines (detailed below), as observed upon examination of any immune parameter in a human population. Indeed, even body weight varied extensively between RIX lines, despite careful age matching (Supp. Table 2, Supp. Fig. 2A). Together, we present an extensive array of steady-state immunity data for each animal in the screen garnered from our three thirteen-color flow cytometry panels as well as clinical observations. Each immune phenotype examined resulted in a high degree of variability by genetic background of the host, and exceeded the breadth of responses observed in the most commonly used inbred strains C57BL/6J and BALB/cJ (Supp. Table 3). Importantly, because our dataset is included (Supp. Table 4) and available on ImmPort, researchers can select from baseline phenotypes of interest for a particular infection or disease in order to perform a small subset of experiments rather than a large, time and resource consuming phenotypic screen. We anticipate that our dataset, along with these accompanying proof-of-concept studies hereby detailing examples of genetic mapping of immune traits of interest, will advance the use of the CC in immunology and genetic mapping studies.

### Variation in T cell frequencies across CC-RIX lines presents mouse models for immunological studies

Previous studies have demonstrated variation in T cell frequencies based on host genetics, though these studies have largely been restricted to a limited number of commonly used inbred strains of mice (Chen et al., 2005; Feuerer et al., 2007; Holler et al., 2007; Mostafavi et al., 2014; Paula et al., 2011; Petkova et al., 2008), (Bogue and Grubb, 2004; Grubb et al., 2004). To put this previously described variation into context of a larger group of mice with increased genetic variation, we examined the frequency of T cell populations in the spleen of 113 CC-RIX lines as compared to the commonly used BALB/cJ and C57BL/6J model strains. We found a high degree of variability in the frequency of CD3<sup>+</sup> T cells based on host genetics, with average frequencies in CC-RIX lines ranging from 16–62% of gated

lymphocytes, whereas C56BL/6J mice had an average frequency of 36.96% and BALB/cJ had an average frequency of 46.4% (Fig. 1A). Within these splenic CD3+ T cell populations, we further examined the frequencies of CD8+ T cells, CD4+ T cells, and also CD4+Foxp3+ regulatory T cells (Treg). Notably, CD8 T cell frequencies in CC-RIX lines ranged from 14.1–65.3% of CD3+ T cells, with C57BL/6J and BALB/cJ average frequencies of 36.6% and 32.1%, respectively (Fig. 1B). The variability in CD4 T cell frequency in the spleen in CC-RIX mice ranged from 27–73.1% of CD3+ T cells, with C57BL/6J and BALB/cJ average frequencies of 58.96% and 64.5%, respectively (Fig. 1C). As expected due to this variability in CD8 and CD4 T cell frequency, there is also extensive diversity in the CD4/CD8 T cell ratio across CC-RIX lines (Supp. Fig. 2B–C). Finally, we quantified the frequency of Tregs as a percentage of CD4+ T cells, and found that CC-RIX lines had a range of 1.8–25.5% Tregs as compared to C57BL/6J and BALB/cJ average frequencies of 10% and 12.5%, respectively (Fig. 1D). Importantly, the variability in Treg frequency modeled by the CC-RIX is similar to that observed in a large human cohort (Fig. 1E), thereby suggesting that the CC improves greatly upon the ability of two common laboratory strains to represent the diversity in T cell frequency observed in humans. In summary, we find that CC-RIX lines display greatly enhanced variation in the frequency of total T cells as well as CD8+, CD4+, and Foxp3+ subsets as compared to traditional inbred models. Further, we propose that this variation will be key to extend immunological mouse models as well as QTL mapping studies to identify genes regulating homeostatic T cell population dynamics and better understand the role that variant immune homeostasis plays on resultant immunological responses.

### Variation in conventional T cell phenotypes across CC-RIX lines

In addition to examining T cell frequencies in mice with distinct CC-RIX genetic backgrounds, we performed an extensive phenotypic analysis of conventional T cells in order to classify them further into subtypes as well as catalog their activation and functional profiles (Supp. Tables 1 & 3). While the full dataset is available on ImmPort (ImmPort accession SDY1176), we here focus on the frequency of Ki67+ CD8 T cells, which indicates recently or actively proliferating cells; CD44+ CD8 T cells, indicating cells that have experienced antigen; CD62L– CD8 T cells, or activated CD8 T cells; as well as the frequency of CD8 T cells that secrete IFN $\gamma$  or IL-17 upon a polyclonal anti-CD3/CD28 stimulation *ex vivo* (Fig. 2A–E). For reference, while C57BL/6J mice had an average of 10.8% of CD8 T cells that were Ki67+ and BALB/cJ had 7.2%, CC-RIX lines ranged from averages of 2.5–22.5% (Fig. 2A), once again providing a much more diverse response which can be used downstream for unique mouse immunology model studies or for QTL mapping. In addition to this heterogeneous response based on host genetics, we additionally identified in CC-RIX lines a wide range of antigen-experienced CD8 T cell frequencies (Fig. 2B), activated CD8 T cells (Fig. 2C), IFN $\gamma$ -secreting CD8 T cells (Fig. 2D), and IL-17-secreting CD8 T cells (Fig. 2E). Importantly, all the mice used within these studies were bred within the same facility and experiments were similarly conducted in a common environment. Together, these data suggest that homeostatic immune responses and the propensity to initiate adaptive immunity is under strong genetic control, and this dataset may thus inform further studies of autoimmunity and tolerance.

Similarly, we examined a wide range of conventional CD4 T cell phenotypes based on cellular expression of activation markers, homing and effector molecules (Supp. Tables 1 & 3). As examples of the phenotypic diversity measured in CD4 T cells across different CC-RIX lines, we demonstrate a large range of Ki67+ CD4 T cells, from 3.8–46.9% of total splenic CD4 T cells, whereas C57BL/6J and BALB/cJ mice had similar average frequencies of 8.9% and 8.5%, respectively (Fig. 2F). Similarly, the fraction of CD4 T cells that were positive for the transcription factor Tbet, and thus likely to be Th1 cells, ranged from nearly 0 to 35.1% across CC-RIX lines, but again C57BL/6J and BALB/cJ mice had similar average frequencies of 2.5% and 2.3%, respectively (Fig. 2G), underscoring the utility of CC-RIX mice to establish unique mouse models of immune phenotypes beyond what can be modeled using C56BL/6J or BALB/cJ mice. Additionally, there are large differences in the frequencies of splenic CD4+ T cells able to secrete IFN $\gamma$  or IL-17 following a polyclonal *ex vivo* stimulus (Fig. 2H–I), as well as antigen-experienced CD44+ or activated CD62L– CD4 T cells (Fig. 2J–K). In conclusion, both this dataset and the CC-RIX are an invaluable resource for investigators looking for an improved mouse model in which to study phenotypic diversity in T cells, as well as for use in genetic mapping studies of T cell phenotypes.

### Genetic variation results in differential immunoregulation

Tregs, defined by the lineage marker forkhead box P3 (Foxp3), promote self-tolerance and limit autoimmunity (Belkaid and Tarbell, 2009; Campbell and Koch, 2011; Kim et al., 2007), and altered Treg function is implicated in the manifestation of many autoimmune syndromes (Buckner, 2010). Most severely, in the complete absence of Tregs, as exemplified by Treg-deficient scurfy mice or individuals carrying non-functional versions of the *Foxp3* gene, life-threatening multi-organ autoimmunity and lymphoproliferative diseases manifest in early development (Brunkow et al., 2001; Gambineri et al., 2003). Given the importance of Tregs in regulating conventional T cells, we extensively examined activation and homing molecule expression patterns on Tregs within CC-RIX lines. Most notably, there is a full range of Treg expression levels of the immunosuppressive marker CD73 across CC-RIX mice, from 3.5–97.8% (Fig. 3A). Similarly, the average frequency of Tregs from CC-RIX lines that expressed CTLA-4, a critical suppressive mechanism, ranged from 11.2–86.2%. Finally, there were wide ranges of Tregs expressing CD44 and homing molecule  $\beta$ 1 integrin (CD29) across CC-RIX lines (Fig. 3C–D). Thus, our thorough analysis demonstrates the variation in Treg-mediated immunoregulation dependent on host genetics, thus providing a rich resource for additional immunoregulatory and immunogenetics research.

Due to the large variation in frequency of Tregs that we observed in overtly healthy and age-matched mice, similar to what has been observed in humans (Fig. 1E), we further interrogated for a possible relationship between the number of Tregs and their suppressive capacity to address the question of whether Treg function could compensate for altered Treg frequency so as to maintain overall health of the host. First, we performed a linear regression analysis of Treg number by CD4+ and CD8+ T cell proliferation, as indicated by Ki67 expression, or activation indicated by CD44 or absence of CD62L expression. There was not a statistically significant correlation between Treg number and T cell proliferation or activation (Supp. Fig. 3), suggesting that mice with varying numbers of Tregs are equally

able to control T cell proliferation and activation. This finding supported our hypothesis that mice with lower Treg numbers may compensate for this by having increased Treg activation or Treg suppressive capacity in order to control immune activation similarly to mice with a higher number of total Tregs. Thus, we tested for correlations between Treg number and the frequency of various Treg activation or suppression markers, and found that there was indeed a statistically significant inverse correlation between the number of Tregs and the frequency of Tregs expressing CTLA-4, CXCR3, or ICOS (Fig. 3E–G). Thus, our data supports a model in which mice with lower numbers of Tregs may compensate for this by having increased activation or suppressive capacity of Tregs in order to maintain tolerance and overall health. Alternatively, mice with less functional or suppressive Tregs may have a compensatory expansion, perhaps because reduced suppression of T cells, mediated by CTLA-4, for example, results in abundance of IL-2 that can thus support expansion of the Treg population. Together, our data demonstrate that mice on different genetic backgrounds support a wide range of Treg frequencies while maintaining health, at least in part by altering the suppressive function of Tregs.

### Mouse model development using the Collaborative Cross

As demonstrated above, there is tremendous phenotypic diversity generated within T cell subsets dependent on the natural standing genetic variation available within the Collaborative Cross. To provide an example of the utility of the CC for development of new mouse models for immunology research, we focused on the extreme diversity observed in the frequency of Tregs (Fig. 1D). The vast majority of research on Tregs over the past 15 years has used C57BL/6J mice, which have a population of Tregs comprising approximately 10% of the total CD4 T cell compartment within the spleen. In order to identify potential mouse models with different Treg frequencies (e.g. akin to the diversity observed in human cohorts (Fig. 1E)), we further examined the frequency of Tregs in CC-RI strains that served as dams or sires in matings that resulted in CC-RIX lines at the extreme ends of Treg frequency depicted in Fig. 1D. We found that CC-RI strains CC030/GeniUnc, CC061/GeniUnc, CC051/TauUnc and CC003/Unc had average Treg frequencies of 12.03%, 7.05%, 8.47%, and 4.66%, respectively (Fig. 3H). Notably, none of these RI lines had Treg frequencies that were elevated or decreased to the extremes observed in the CC-RIX screen, although CC030 does have a consistently lower frequency of Tregs and might represent a model of decreased Treg activity. These results highlight the potential for emergent phenotypes within heterozygous animals (e.g. due to epistatic genetic interactions), and further underscore the utility of assessing F1 crosses to increase both the genetic and phenotypic diversity assessed.

### Quantitative trait loci mapping using the Collaborative Cross

The Collaborative Cross was initially conceived of as a powerful resource for genetic mapping studies and integrated systems genetics approaches (Churchill et al., 2004). To measure the amount of phenotypic variation attributable to genetic differences, we calculated the intraclass correlation (ICC) (Gelman and Hill, 2007) measures as an estimate of heritability (Supplemental Table 4). In addition, to demonstrate the overall immune system phenotypic diversity among CC-RIX lines, we performed principal component analysis (PCA) using the flow cytometry measures listed in Supplemental Table 4 (using strain

average values), and then plotted the top two PCs to show strain clustering within these composite immune phenotypes (Supp Fig. 4). This analysis demonstrates that there is tremendous overall immune system phenotypic diversity across the CC-RIX, and not just diversity within single immune measures, as demonstrated in Figs. 1–3. Further, while there is diversity among the lines with regard to multiple different cell populations, there are also a number of lines with quite extreme phenotypes, which may thus be suitable for follow-up studies.

Next, to demonstrate the utility of the CC for identifying QTL contributing to population-wide variation in steady-state immune phenotypes, we performed QTL mapping on select T cell phenotypes using our flow cytometry data in combination with haplotype reconstructions of the CC strains generated from the mouse universal genotyping array (Mega-MUGA) platform (Morgan et al., 2015). Through these proof-of-concept studies, we identified several QTL candidates for follow-up, and below we highlight examples chosen due to high LOD scores and clear founder effects. First, we found a QTL (Host Immunity 1, *H1I*) driving the frequency of CD73+ Tregs within the X-chromosome near position 160Mb-telomere (Fig. 4A) that appears to be driven largely by a PWK/PhJ founder effect (Fig. 4B). Confirming this locus, those CC-RIX lines with a PWK/PhJ haplotype at position 166Mb of the X-chromosome have frequencies of CD73+ Tregs that are on the upper end of the range we observed across all CC-RIX examined (Fig. 4C and 3A). This has clear implications on host immunoregulation at steady-state as there is an inverse correlation between CD73+ Treg frequency and the frequency of activated CD8 or CD4 T cells (Fig. 4D).

In an effort to narrow our QTL regions to likely candidate genes, we utilized whole genome sequence information from the 8 founder strains of the CC (Keane et al., 2011). Guided by the allele effects underlying the QTL analysis (estimates of which founder haplotype(s) causative genetic variants occur in), we sought to identify genetic variants within the QTL regions that were (a) consistent with allele effects underlying the QTL, and (b) also had an impact on the amino acid sequence and/or splice forms of a gene, as these variants would be the highest priority candidates for altering protein function. Accordingly, within the QTL, a total of 102,596 SNPs and 20,432 insertions/deletions (InDels) segregate across the CC population. Of these, 248 SNPs and 14 InDels cause coding or splice differences across 43 genes. Since a PWK/PhJ allele was the sole allele contributing to phenotypic differences, we focused on private PWK/PhJ variants. We identified 36 private PWK/PhJ SNPs and 2 InDels within 22 genes (Table 1) as potential causal candidates.

In addition to this QTL, we also identified a highly significant QTL (*H12*) within the X-chromosome at position 100–106 Mb driving the frequency of CXCR3+ Tregs (Fig. 5A), CXCR3+ CD4+, and CD8+ T cells (data not shown). When we examined the founder effects, we found that PWK/PhJ again was a significant driver of this QTL for all three phenotypes (Fig. 5B and data not shown), with a clear trend toward low levels of CXCR3 expression on all three subsets of T cells of CC-RIX lines when there were PWK/PhJ variants at position 105.5Mb on the X-chromosome (Fig. 5C–D and data not shown). However, this QTL had a more complex pattern of allele effects depending on the phenotype. While in all cases a PWK/PhJ allele drives a decreased frequency of CXCR3+ T cells for any of the three subsets of T cells, there is additional evidence for phenotype-



specific allele effects leading to increases in frequency of each of these specific cell types. Specifically, there is a WSB/EiJ haplotype associated with increased CXCR3<sup>+</sup> CD8<sup>+</sup> T cells, and also a NZO/HILtJ haplotype increasing CXCR3<sup>+</sup> Tregs (Fig. 5B and 5E). In this 6 Mb region, a total of 55082 SNPs and 12377 InDels segregate within the CC. This includes 149 nonsynonymous SNPs and 11 InDels across 42 genes. PWK has 35 private SNPs and 5 private InDels in 26 genes; NZO has 4 SNPs and 1 InDel in 4 genes (Table 1). WSB/EiJ has no private SNPs or InDels within this region, suggesting effects of the WSB/EiJ haplotype may be due to regulatory variation. Of note, genes within this X-chromosome QTL driving low frequency of CXCR3<sup>+</sup> T cells include *Cxcr3* itself (Table 1), thereby likely demonstrating novel gene variants that result in altered expression levels within T cells. CXCR3 is a critical chemokine receptor used by T cells and other immune cells to migrate to tissue sites of infection and sites of autoimmune reactions, and Tbet<sup>+</sup> CXCR3<sup>+</sup> Tregs have been shown to provide protection from autoimmune diabetes (Tan et al., 2016). Further study of CC-RI or CC-RIX with the PWK/PhJ haplotype in this region could better model human disease associated with altered T cell migratory activity, and also be used to study the importance and function of this chemokine receptor itself.

Finally, we identified a third candidate QTL within the X-chromosome at position 140–145 Mb (*Hl3*) driving the frequency of ICOS<sup>+</sup> Tregs in the spleen (Fig. 6A). While this ICOS<sup>+</sup> Treg result does not meet the threshold for statistical significance in our analysis, the allele effects are clear and we include it here as an example of the diverse allele effects seen in the RIX population. An examination of the founder allele effects at this locus revealed that the PWK/PhJ haplotype was associated with an increased frequency of ICOS<sup>+</sup> Tregs (Fig 6B–C), thereby accounting for the extreme frequency at the higher ranges (Fig. 6D). However, there also appeared to be a second, NZO/HILtJ allele which had an intermediate increase in ICOS<sup>+</sup> Tregs relative to the other six haplotypes (Fig. 6B). Within this region there are a total of 51,137 SNPs and 10,884 InDels segregating in the CC. Of these, 58 SNPs and 5 InDels cause coding or splice differences in 18 genes. PWK/PhJ has 17 private SNPs and 2 private InDels across 11 genes (Table 1). In contrast, NZO/HILtJ has no SNPs or InDels either private or shared with PWK/PhJ in this region, suggesting the potential for regulatory variants to play a role in this locus. In summary, we hereby highlight examples of QTL analysis for immunoregulatory phenotypes at homeostasis, with several potential candidate genes under the QTL identified for follow-up studies.

## Discussion

The highly genetically diverse Collaborative Cross was conceived of as an experimental system which could be used to understand how genetic variation could impact a variety of complex traits, while still maintaining the benefit of reproducibility and the legion of other advantages of a small animal model, such as controlled environment, diet, age, sex, and pathogen exposure. An early study using individual mice from 66 strains from incipient lines of the CC, or pre-CC, demonstrated diversity in the steady-state frequency of subsets of lymphocytes and antigen-presenting cells that was larger than that detected in the eight founder strains (Phillippi et al., 2014); here, we use the completed CC to extend these initial observations using replicate animals and a wider and comprehensive range of phenotypic analyses. A number of studies have shown that genetic variants circulating within the CC

population can lead to divergent responses to pathogens (Elbaheesh and Schughart, 2016; Ferris et al., 2013; Graham et al., 2016; Graham et al., 2015; Gralinski et al., 2015; Leist et al., 2016; Lore et al., 2015; Rasmussen et al., 2014), inflammatory diseases (Rogala et al., 2014), and drug responses (Nachshon et al., 2016). Here, we advance and expand on this growing body of work, with a demonstration of the unique benefits for immunology research. CC-RI and CC-RIX lines can provide exciting new and reproducible models for cellular immunology research, as well as provide us with a critical resource for mapping immune phenotypes to genetic loci and genes.

Importantly, each cellular immune phenotype that we examined as part of our screen resulted in a wide range of responses at homeostasis, with increased diversity beyond the most commonly used laboratory inbred strains of C56BL/6J and BALB/cJ. This consistent range of differences between CC recombinant inbred lines extends our ability to model human diversity in T cell frequency and phenotype, and potentially the unique resultant infection or disease outcomes, such as autoimmunity. For example, CC-RIX lines or CC-RI strains at the tails of the phenotypic distribution plots are useful for elucidating the underlying mechanisms of the high or low phenotype of interest. For example, as identified in Fig. 3H, CC-RI strain CC003/Unc and CC-RIX lines (CC003xCC062) and (CC070xCC003) all have splenic Treg frequencies that are about half that measured in C57BL/6J mice (Fig. 1D), although these lines are all overtly healthy and display no signs of autoimmunity within the 8–10 week age range. It has been previously noted that BALB/c mice have more CD4+CD25+ Tregs as compared to C57BL/6 mice, including greater suppression of their CD4+CD25– responder T cells (Chen et al., 2005), but the genetic loci regulating this difference were not identified. Here we confirm this finding of differential Treg frequency between Balb/cJ and C57BL/6J as well as within the CC-RIX (Fig. 1D), although due to the large and high-throughput nature of our screen, we cannot draw conclusions about the suppressive capacity of the Tregs across the CC-RIX lines, as *in vitro* suppression assays were not performed for each of the lines screened. Important follow-up studies include an examination of Treg suppressive capacity through use of standard suppression assays to determine if any of the CC-RIX lines represent unique mouse models of extreme immunoregulation mediated by Treg suppression. Further, such studies could be used to map the gene(s) responsible for differential Treg activity, which could have critical downstream implications for susceptibility to infection, autoimmunity, and tumorigenesis.

In addition to provision of mouse models for cell-type and disease-specific research, we hereby demonstrate that the T cell phenotypic diversity present within the CC affords us with an unprecedented ability to perform genetic mapping to identify loci controlling adaptive immune phenotypes and responses. Through the proof-of-concept QTL analyses performed by our group (Figs. 4–6), we identified 3 QTL underlying distinct immunoregulatory phenotypes at steady-state. Our ability to identify effects on the X chromosome was increased compared to autosomes because our mapping population consists of males only. In this case, significance thresholds for the X chromosome are somewhat lower than for autosomes due to the hemizygous genotypes of males, as there are no heterozygotes. Notably, a candidate gene under the X-chromosome QTL driving very low expression of CXCR3 on Tregs, CD4, and CD8 T cells is *Cxcr3* itself, suggestive of a deleterious allele resulting in lowered levels of protein expression. Since CXCR3 is a

chemokine receptor important for lymphocyte migration toward chemokines CXCL9, CXCL10, and CXCL10, which are generally expressed in tissue regions of inflammation (Groom and Luster, 2011), mouse lines with this allele may represent a unique model in which to study the importance of this signaling pathway in various disease or infection states. In humans, CXCR3 polymorphisms have been associated with the risk of asthma (Cheong et al., 2005), pointing to a potential future use of the CC-RIX to improve mouse models of asthma research to better recapitulate human disease states. Additionally, the list of candidate genes provided in Table 1 requires follow-up studies in order to narrow in on the particular gene or genes causing the phenotypes of interest.

Genetic variants driving phenotypic differences can be due to both coding and regulatory differences. Indeed, many of the most significant human GWAS hits occur in regulatory regions (Zhang and Lupski, 2015). Here, we present an initial analysis where we instead focused on variants impacting protein sequence. Many studies in the CC have shown that differences in coding sequence can have large effects on phenotypic outcomes (Ferris et al., 2013; Gralinski et al., 2015). Furthermore, regulatory variants are notoriously difficult to identify due to their condition and cell-type specific effects on gene expression, which itself does not always lead to differences in protein levels (Chick et al., 2016). Nevertheless, differentiating between protein functional and expression level differences in phenotypic responses provides critical hypotheses to address in future studies of the functions of variant regions on immune homeostasis.

Our study and the power of our dataset have several limitations. First, we cannot determine a role for distinct microbiota within CC-RIX lines or animals in driving some of the divergent immune phenotypes. Mice of different lines were not co-housed or co-fostered, although they were all bred within the same room of the same facility by the same technician across the entire study. Similarly, experiments were conducted within a consistent facility, so together these factors should minimize the impact of a variety of environmental factors. However, the microbiome could explain some of the observed variation, and while a study of this magnitude, performed over the course of 4 years, did not allow for an extensive examination of the microbiome as well, future studies will likely investigate the role of host genetics on microbiome colonization, as well as downstream effects of distinct microbial communities on immune phenotypes. An additional limitation of our study is that haplotype blocks are fairly large within this CC-RIX population. However, in contrast to classical 2-allele mapping populations, the multiple founder haplotypes do allow us to reduce large haplotype blocks to much fewer numbers of candidate features, which we did here as an illustrative example of the use of this Resource and dataset.

In conclusion, we hereby advance that the Collaborative Cross is an invaluable resource for many types of immunology, immunogenetics, and disease research, as we have specifically demonstrated in the context of steady-state T cell phenotypes and frequencies. This dataset will be useful for individuals seeking to identify new mouse models with increased diversity of T cell phenotypes more akin to human diversity, as well as for additional QTL mapping studies. Finally, the data presented here provide a gateway for CC strain selection for future studies of cancer immunity, autoimmune conditions, and various infections, as investigators can tailor selection of strains based on the frequencies of particular T cell subsets, as well as

their activation status, steady-state cytokine expression, and other phenotypic selection parameters (Supp. Tables 1 & 4). As the need for mechanistic studies of immunity and disease persists, including the genetic mechanisms underlying such states, we propose that the Collaborative Cross represents an outstanding and unique model that incorporates genetic diversity while at the same time retaining beneficial features of mouse models such as reproducibility, low-cost, and ubiquity and availability of reagents and tools.

## Experimental Procedures

### Mice

CC RI mice were obtained from the Systems Genetics Core Facility at the University of North Carolina-Chapel Hill (UNC) (Welsh et al., 2012). For the screen, CC RIX lines were bred at UNC under specific pathogen free conditions. 6–8 week old F1 hybrid male mice were transferred from UNC to the University of Washington and housed directly into a BSL-2+ laboratory within an SPF barrier facility. Age- and sex-matched eight to ten week old mice were used for all experiments. All animal experiments were approved by the University of Washington Institutional Animal Care and Use Committee. The Office of Laboratory Animal Welfare of the National Institutes of Health (NIH) has approved UNC (#A3410-01) and the University of Washington (#A3464-01), and this study was carried out in strict compliance with the Public Health Service (PHS) Policy on Humane Care and Use of Laboratory Animals. Genotypes of interest in this study, *H2b*, were obtained from the Systems Genetics Core Facility at UNC (Welsh et al., 2012).

### Cell preparation for flow cytometry assays

Following euthanasia, mice were perfused with 10 ml PBS to remove any residual intravascular leukocytes. Spleens were homogenized, treated with ACK lysis buffer to remove red blood cells, washed, and resuspended in FACS buffer (1X PBS, 0.5% FBS). Cells were counted by hemacytometer using trypan blue exclusion.

### Flow cytometry analysis

Following preparation of single cell suspensions, cells were plated at  $1 \times 10^6$  cells/well and stained for surface markers for 15 minutes on ice. Cells were subsequently fixed, permeabilized (Foxp3 Fixation/Permeabilization Concentrate and Diluent, Ebioscience) and stained intracellularly with antibodies for 30 minutes on ice. Flow cytometry was performed on a BD LSR II machine using BD FACSDiva software. Analysis was performed using FlowJo software. The following directly conjugated antibodies were used: CD3-ECD (145-2C11), CD4-BV605 (RM4-5), CD8-BV650 (53-6.7), Foxp3-Alexa700 (FJK-16S), CD44-FITC (IM7), CD62L-Alexa700 (MEL-14), IFN $\gamma$ -PerCP eFluor710 (XMG1.2), IL-17-FITC (TC11-18H10.1), Tbet-PECy7 (4B10), CD73-BV421 (TY/11.8), CTLA-4-APC (UC10-4B9), ICOS-PECy5 (7E.17G9), CD29-APC Cy7 (HMb1-1), CXCR3-PerCP eFluor710 (CXCR3-173), and Ki67-FITC (SolA15). AmCyan Live/dead stain (Invitrogen) was used in all panels for identification of live cells. Gating schemes and trees used for flow cytometry analysis are shown in Supplementary Figure 1. To measure the amount of phenotypic variation attributable to genetic differences, intraclass correlation (ICC) values were calculated for all flow measures (Gelman and Hill, 2007).

## Measurement of human Treg frequency

Cryopreserved PBMCs were obtained from individuals participating in the Partners PrEP Study (ClinicalTrials.gov number NCT00557245). Study procedures have been described previously (Baeten et al., 2012). For the present analysis, samples were selected from men and women who were HIV-negative. The procedures of the Partners PrEP Study, including collection of samples for immunologic assays, were approved by the institutional review boards of the University of Washington and collaborating site institutions; participants provided written informed consent.

PBMCs from 244 individuals were thawed and cultured in R10. Counts and viability were acquired using the TC-20 Automated Cell Counter (Bio-Rad Laboratories, Inc.). Tregs were stained with Live/Dead Fixable Aqua Dead Cell Stain Kit from Molecular Probes (OR, USA), followed by cell surface staining with the appropriate cell panel. Surface markers examined for phenotype staining protocol include: CD3 (OKT3 and HIT3a), CD4 (OKT4), CD25 (BC96), CD127 (A019D5) from Biolegend, Inc. (CA, USA); CD8 (SK1) from eBioscience, Inc. (CA, USA). Intracellular markers examined include FoxP3 (236 A/E7) from ebioscience, Inc. (CA, USA). Immediately following staining, samples were analyzed using a LSRII flow cytometer (BD Biosciences, CA, USA) with FlowJo software (Treestar, Inc, OR). Tregs were considered to be CD3+CD4+CD25hiFoxp3+CD127dim cells, as previously published (Pattacini et al., 2016).

## Statistical analysis

When comparing groups, two-tailed unpaired Student's *t* tests were conducted, with *p*-values <0.05 considered significant. Error bars show +/- SEM or +/- SD.

## Principal Component Analysis

Principal component analysis (PCA) was performed using all measures listed in Supplemental Table 4. For all measures, average values for each CC RIX line were calculated. The proportion of missing values was examined for each CC RIX line and each flow cytometry measure. CC RIX lines and measures with greater than 15% missing values were excluded from the analysis. The remaining missing values were replaced with the average value across all lines. Finally, each measure was scaled and centered before performing PCA.

## Calculation of ICC (estimate of heritability)

A random effects model was fit for each flow variable:

$$y_{ij} = \mu + \alpha_j + \epsilon_{ij}$$

where  $y_{ij}$  is the *i*-th observation for *j*-th group,  $\mu$  is the overall mean,  $\alpha_j$  is a random effect, and  $\epsilon_{ij}$  is the error. ICC is defined below, where  $\sigma^2\alpha$  is the variance explained by the grouping factor (RIX line) and  $\sigma^2\epsilon$  is the variance not explained by the grouping factor.

$$ICC = \sigma^2 \sigma / (\sigma^2 \sigma + \sigma^2 \varepsilon)$$

### Quantitative Trait Loci Mapping

QTL mapping was done as previously described (Aylor et al., 2011; Ferris et al., 2013). Briefly, the haplotypic makeup of each CC-RIX was determined based on the consensus most recent common ancestor (MRCA) for each CC-RI line. As each RIX is an F1, the haplotype probabilities were averaged between the two strains for each of the autosomes, whereas the X chromosome for each RIX was determined solely with the mother strain's haplotypic makeup (as these CC-RIX were males, they all have one copy of the X chromosome inherited from their dam). The DOQTL package conducts an eight-variable (the probability of each of the eight founder haplotypes at a locus) regression on probabilities framework at each marker of interest, looking to find significant associations between the founder haplotype probabilities at a marker with the associated phenotypes present within the RIX. Genome-wide significance is determined by permutation testing (randomly shuffling the phenotypic values across the CC-RIX and asking for the most significant response value). Allele effects at each locus are determined by taking the effect estimate for each of the eight founder haplotypes (the  $\beta$  within a linear regression framework).

In order to determine likely causative variants at a locus, we used the allele effects to identify the largest split between effects at a QTL. When there were two splits of roughly equal magnitude, then we assumed that there were 3 allele groups with a more complex SNP pattern. We took all of the called genetic variants within the QTL based on the sanger whole genome sequences of the eight founder strains, and looked at the variant distribution pattern. As described in the results, we filtered these variants based on potential impact on protein sequence to derive lists of higher priority candidate genes.

An additive haplotype regression model implemented in the DOQTL R (Team, 2016) package was used for QTL mapping analyses (Gatti et al., 2014). Briefly, QTL genome scans are performed by regressing the phenotype on genotype probabilities for each of the eight founder strains. A random-effect term is included in the model to account for kinship among animals. The DOQTL software also requires sex to be included as a covariate in the regression model, although all our samples are male. A LOD score for each marker is calculated from the likelihood ratio comparing the regression model described above to a regression model without the founder genotype probabilities. The statistical significance of LOD scores is determined via a permutation test. A threshold of  $p \leq 0.05$  was used to select significant associations.

### Data availability

The data that support the findings of this study are included in Supplementary files and are available via ImmPort (accession SDY1176).

## Supplementary Material

Refer to Web version on PubMed Central for supplementary material.

## Acknowledgments

Funding for this study was provided by NIH grant U19AI100625 (Project 4 and Cores C and D) to MTF, SM and JML and NIH grants R01 AI096968 and AI087657 to JML. We wish to thank our collaborators in the Systems Immunogenetics Group for helpful discussions and generation of mice. In particular, we wish to thank Ginger Shaw for generating the RIX mice used in this study. The authors declare no conflicts of interest.

## References

- Aylor DL, Valdar W, Foulds-Mathes W, Buus RJ, Verdugo RA, Baric RS, Ferris MT, Frelinger JA, Heise M, Frieman MB, et al. Genetic analysis of complex traits in the emerging Collaborative Cross. *Genome Res.* 2011; 21:1213–1222. [PubMed: 21406540]
- Baeten JM, Donnell D, Ndase P, Mugo NR, Campbell JD, Wangisi J, Tappero JW, Bukusi EA, Cohen CR, Katabira E, et al. Antiretroviral prophylaxis for HIV prevention in heterosexual men and women. *The New England journal of medicine.* 2012; 367:399–410. [PubMed: 22784037]
- Belkaid Y, Tarbell K. Regulatory T cells in the control of host-microorganism interactions (\*). *Annual review of immunology.* 2009; 27:551–589.
- Bogue MA, Grubb SC. The Mouse Phenome Project. *Genetica.* 2004; 122:71–74. [PubMed: 15619963]
- Boguski MS. Comparative genomics: the mouse that roared. *Nature.* 2002; 420:515–516. [PubMed: 12466847]
- Brunkow ME, Jeffery EW, Hjerrild KA, Paeper B, Clark LB, Yasayko SA, Wilkinson JE, Galas D, Ziegler SF, Ramsdell F. Disruption of a new forkhead/winged-helix protein, scurfy, results in the fatal lymphoproliferative disorder of the scurfy mouse. *Nat Genet.* 2001; 27:68–73. [PubMed: 11138001]
- Buckner JH. Mechanisms of impaired regulation by CD4(+)CD25(+)FOXP3(+) regulatory T cells in human autoimmune diseases. *Nature reviews Immunology.* 2010; 10:849–859.
- Campbell DJ, Koch MA. Phenotypical and functional specialization of FOXP3+ regulatory T cells. *Nature reviews Immunology.* 2011; 11:119–130.
- Chen X, Oppenheim JJ, Howard OM. BALB/c mice have more CD4+CD25+ T regulatory cells and show greater susceptibility to suppression of their CD4+CD25– responder T cells than C57BL/6 mice. *Journal of leukocyte biology.* 2005; 78:114–121. [PubMed: 15845645]
- Cheong HS, Park CS, Kim LH, Park BL, Uh ST, Kim YH, Lym GI, Lee JY, Lee JK, Kim HT, et al. CXCR3 polymorphisms associated with risk of asthma. *Biochem Biophys Res Commun.* 2005; 334:1219–1225. [PubMed: 16043121]
- Chesler EJ. Out of the bottleneck: the Diversity Outcross and Collaborative Cross mouse populations in behavioral genetics research. *Mamm Genome.* 2014; 25:3–11. [PubMed: 24272351]
- Chick JM, Munger SC, Simecek P, Huttlin EL, Choi K, Gatti DM, Raghupathy N, Svenson KL, Churchill GA, Gygi SP. Defining the consequences of genetic variation on a proteome-wide scale. *Nature.* 2016; 534:500–505. [PubMed: 27309819]
- Churchill GA, Airey DC, Allayee H, Angel JM, Attie AD, Beatty J, Beavis WD, Belknap JK, Bennett B, Berrettini W, et al. The Collaborative Cross, a community resource for the genetic analysis of complex traits. *Nat Genet.* 2004; 36:1133–1137. [PubMed: 15514660]
- Collaborative Cross, C. The genome architecture of the Collaborative Cross mouse genetic reference population. *Genetics.* 2012; 190:389–401. [PubMed: 22345608]
- Elbahesh H, Schughart K. Genetically diverse CC-founder mouse strains replicate the human influenza gene expression signature. *Sci Rep.* 2016; 6:26437. [PubMed: 27193691]
- Ferris MT, Aylor DL, Bottomly D, Whitmore AC, Aicher LD, Bell TA, Bradel-Tretheway B, Bryan JT, Buus RJ, Gralinski LE, et al. Modeling host genetic regulation of influenza pathogenesis in the collaborative cross. *PLoS Pathog.* 2013; 9:e1003196. [PubMed: 23468633]

- Feuerer M, Jiang W, Holler PD, Satpathy A, Campbell C, Bogue M, Mathis D, Benoist C. Enhanced thymic selection of FoxP3+ regulatory T cells in the NOD mouse model of autoimmune diabetes. *Proceedings of the National Academy of Sciences of the United States of America*. 2007; 104:18181–18186. [PubMed: 17991775]
- Gambineri E, Torgerson TR, Ochs HD. Immune dysregulation, polyendocrinopathy, enteropathy, and X-linked inheritance (IPEX), a syndrome of systemic autoimmunity caused by mutations of FOXP3, a critical regulator of T-cell homeostasis. *Curr Opin Rheumatol*. 2003; 15:430–435. [PubMed: 12819471]
- Gatti DM, Svenson KL, Shabalin A, Wu LY, Valdar W, Simecek P, Goodwin N, Cheng R, Pomp D, Palmer A, et al. Quantitative trait locus mapping methods for diversity outbred mice. *G3 (Bethesda)*. 2014; 4:1623–1633. [PubMed: 25237114]
- Gelman, A., Hill, J. *Data analysis using regression and multilevel/hierarchical models*. Cambridge; New York: Cambridge University Press; 2007.
- Gondo Y, Fukumura R, Murata T, Makino S. ENU-based gene-driven mutagenesis in the mouse: a next-generation gene-targeting system. *Exp Anim*. 2010; 59:537–548. [PubMed: 21030782]
- Graham JB, Swarts JL, Wilkins C, Thomas S, Green R, Sekine A, Voss KM, Ireton RC, Mooney M, Choonoo G, et al. A Mouse Model of Chronic West Nile Virus Disease. *PLoS Pathog*. 2016
- Graham JB, Thomas S, Swarts J, McMillan AA, Ferris MT, Suthar MS, Treuting PM, Ireton R, Gale M Jr, Lund JM. Genetic diversity in the collaborative cross model recapitulates human West Nile virus disease outcomes. *MBio*. 2015; 6:e00493–00415. [PubMed: 25944860]
- Gralinski LE, Ferris MT, Aylor DL, Whitmore AC, Green R, Frieman MB, Deming D, Menachery VD, Miller DR, Buus RJ, et al. Genome Wide Identification of SARS-CoV Susceptibility Loci Using the Collaborative Cross. *PLoS Genet*. 2015; 11:e1005504. [PubMed: 26452100]
- Groom JR, Luster AD. CXCR3 ligands: redundant, collaborative and antagonistic functions. *Immunology and cell biology*. 2011; 89:207–215. [PubMed: 21221121]
- Grubb SC, Churchill GA, Bogue MA. A collaborative database of inbred mouse strain characteristics. *Bioinformatics*. 2004; 20:2857–2859. [PubMed: 15130929]
- Holler PD, Yamagata T, Jiang W, Feuerer M, Benoist C, Mathis D. The same genomic region conditions clonal deletion and clonal deviation to the CD8alphaalpha and regulatory T cell lineages in NOD versus C57BL/6 mice. *Proceedings of the National Academy of Sciences of the United States of America*. 2007; 104:7187–7192. [PubMed: 17438291]
- Keane TM, Goodstadt L, Danecek P, White MA, Wong K, Yalcin B, Heger A, Agam A, Slater G, Goodson M, et al. Mouse genomic variation and its effect on phenotypes and gene regulation. *Nature*. 2011; 477:289–294. [PubMed: 21921910]
- Kim JM, Rasmussen JP, Rudensky AY. Regulatory T cells prevent catastrophic autoimmunity throughout the lifespan of mice. *Nat Immunol*. 2007; 8:191–197. [PubMed: 17136045]
- Leist SR, Pilzner C, van den Brand JM, Dengler L, Geffers R, Kuiken T, Balling R, Kollmus H, Schughart K. Influenza H3N2 infection of the collaborative cross founder strains reveals highly divergent host responses and identifies a unique phenotype in CAST/EiJ mice. *BMC Genomics*. 2016; 17:143. [PubMed: 26921172]
- Lore NI, Iraqi FA, Bragonzi A. Host genetic diversity influences the severity of *Pseudomonas aeruginosa* pneumonia in the Collaborative Cross mice. *BMC Genet*. 2015; 16:106. [PubMed: 26310945]
- Masopust D, Sivula CP, Jameson SC. Of Mice, Dirty Mice, and Men: Using Mice To Understand Human Immunology. *Journal of immunology*. 2017; 199:383–388.
- Morgan AP, Fu CP, Kao CY, Welsh CE, Didion JP, Yadgary L, Hyacinth L, Ferris MT, Bell TA, Miller DR, et al. The Mouse Universal Genotyping Array: From Substrains to Subspecies. *G3 (Bethesda)*. 2015; 6:263–279. [PubMed: 26684931]
- Mostafavi S, Ortiz-Lopez A, Bogue MA, Hattori K, Pop C, Koller D, Mathis D, Benoist C. Immunological Genome, C. Variation and genetic control of gene expression in primary immunocytes across inbred mouse strains. *Journal of immunology*. 2014; 193:4485–4496.
- Mountz JD, Van Zant GE, Zhang HG, Grizzle WE, Ahmed R, Williams RW, Hsu HC. Genetic dissection of age-related changes of immune function in mice. *Scand J Immunol*. 2001; 54:10–20. [PubMed: 11439143]



- Nachshon A, Abu-Toamih Atamni HJ, Steuerman Y, Sheikh-Hamed R, Dorman A, Mott R, Dohm JC, Lehrach H, Sultan M, Shamir R, et al. Dissecting the Effect of Genetic Variation on the Hepatic Expression of Drug Disposition Genes across the Collaborative Cross Mouse Strains. *Front Genet.* 2016; 7:172. [PubMed: 27761138]
- Pattacini L, Baeten JM, Thomas KK, Fluharty TR, Murnane PM, Donnell D, Bukusi E, Ronald A, Mugo N, Lingappa JR, et al. Regulatory T-Cell Activity But Not Conventional HIV-Specific T-Cell Responses Are Associated With Protection From HIV-1 Infection. *Journal of acquired immune deficiency syndromes.* 2016; 72:119–128. [PubMed: 26656786]
- Paula MO, Fonseca DM, Wovk PF, Gembre AF, Fedatto PF, Sergio CA, Silva CL, Bonato VL. Host genetic background affects regulatory T-cell activity that influences the magnitude of cellular immune response against *Mycobacterium tuberculosis*. *Immunology and cell biology.* 2011; 89:526–534. [PubMed: 20956987]
- Petkova SB, Yuan R, Tsaih SW, Schott W, Roopenian DC, Paigen B. Genetic influence on immune phenotype revealed strain-specific variations in peripheral blood lineages. *Physiological genomics.* 2008; 34:304–314. [PubMed: 18544662]
- Phillippi J, Xie Y, Miller DR, Bell TA, Zhang Z, Lenarcic AB, Aylor DL, Krovi SH, Threadgill DW, de Villena FP, et al. Using the emerging Collaborative Cross to probe the immune system. *Genes Immun.* 2014; 15:38–46. [PubMed: 24195963]
- Rasmussen AL, Okumura A, Ferris MT, Green R, Feldmann F, Kelly SM, Scott DP, Safronetz D, Haddock E, LaCasse R, et al. Host genetic diversity enables Ebola hemorrhagic fever pathogenesis and resistance. *Science.* 2014; 346:987–991. [PubMed: 25359852]
- Reilly KM. Using the Collaborative Cross to Study the Role of Genetic Diversity in Cancer-Related Phenotypes. *Cold Spring Harb Protoc.* 2016; 2016.pdb.prot079178.
- Rogala AR, Morgan AP, Christensen AM, Gooch TJ, Bell TA, Miller DR, Godfrey VL, de Villena FP. The Collaborative Cross as a resource for modeling human disease: CC011/Unc, a new mouse model for spontaneous colitis. *Mamm Genome.* 2014; 25:95–108. [PubMed: 24487921]
- Salveti M, Ristori G, Bomprezzi R, Pozzilli P, Leslie RD. Twins: mirrors of the immune system. *Immunol Today.* 2000; 21:342–347. [PubMed: 10871876]
- Tan TG, Mathis D, Benoist C. Singular role for T-BET+CXCR3+ regulatory T cells in protection from autoimmune diabetes. *Proceedings of the National Academy of Sciences of the United States of America.* 2016; 113:14103–14108. [PubMed: 27872297]
- Team, RC. R: A language and environment for statistical computing. Vienna, Austria: R Foundation for Statistical Computing; 2016.
- Threadgill DW, Churchill GA. Ten years of the collaborative cross. *G3 (Bethesda).* 2012; 2:153–156. [PubMed: 22384393]
- Threadgill DW, Miller DR, Churchill GA, de Villena FP. The collaborative cross: a recombinant inbred mouse population for the systems genetic era. *ILAR J.* 2011; 52:24–31. [PubMed: 21411855]
- Welsh CE, Miller DR, Manly KF, Wang J, McMillan L, Morahan G, Mott R, Iraqi FA, Threadgill DW, de Villena FP. Status and access to the Collaborative Cross population. *Mamm Genome.* 2012; 23:706–712. [PubMed: 22847377]
- Yates L, McMurray F, Zhang Y, Greenfield A, Moffatt M, Cookson W, Dean C. ENU mutagenesis as a tool for understanding lung development and disease. *biochem Soc Trans.* 2009; 37:838–842. [PubMed: 19614604]
- Zhang F, Lupski JR. Non-coding genetic variants in human disease. *Hum Mol Genet.* 2015; 24:R102–110. [PubMed: 26152199]

### Highlights

- The Collaborative Cross models the phenotypic diversity observed in human immunity
- QTL mapping in the CC reveals candidate genes linked to T-cell phenotypes

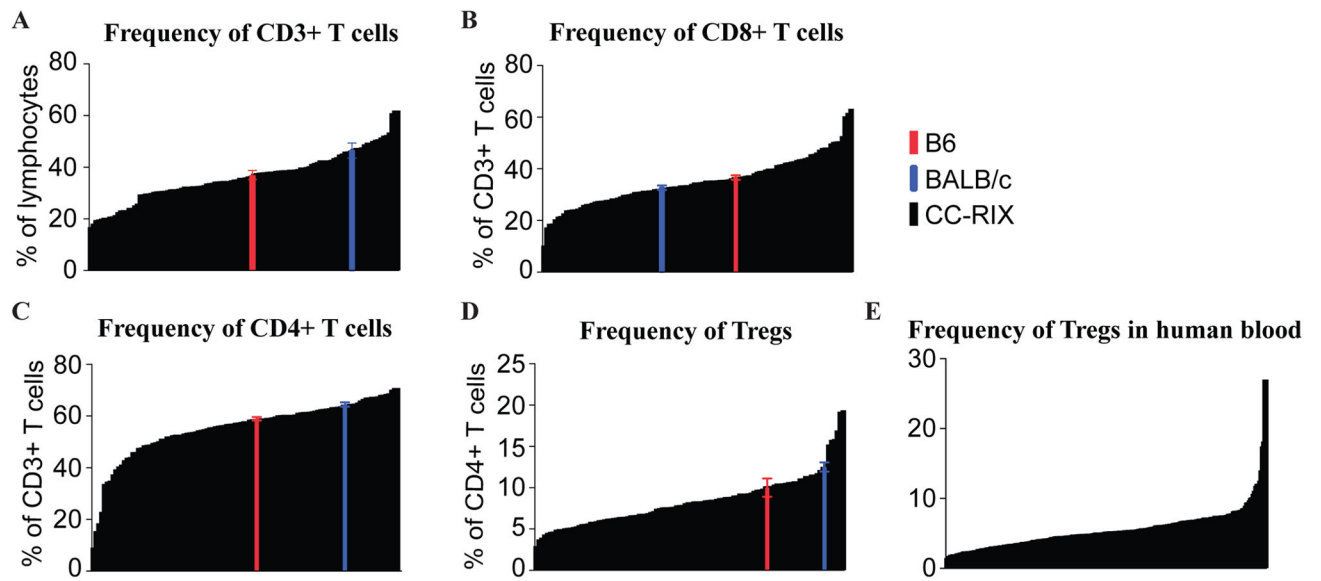


**Figure 1. Variation in frequency of T cell populations at steady state**

Frequencies of CD3+ cells (A), CD8+ cells (B), CD4+ cells (C), and Treg+ cells (D) are plotted for the 110 cohorts of CC mice screened during the discovery phase of the experiment. The average value for the indicated phenotype of each CC RIX line (n=3) is plotted in black in ascending order on the x axis. B6(red) and BALB/c (blue) baseline values are plotted for comparison. All values represent uninfected controls. (E) Frequency of Tregs in human blood from 244 individuals.

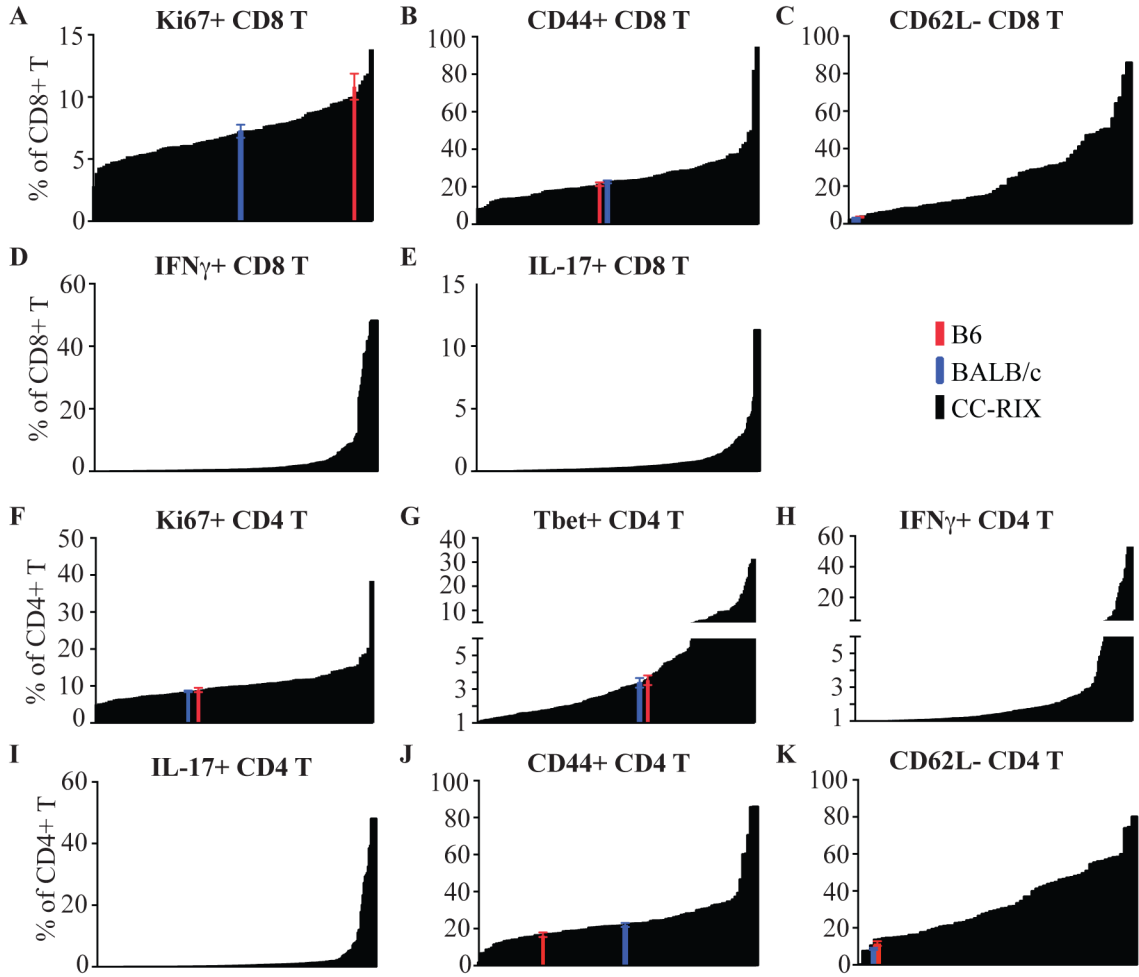


**Figure 2. Variation in conventional T cell phenotypes across CC-RIX lines**

Further analysis of cells subtypes, activation status, and functional profiles across CC-RIX at steady state. Frequencies of CD8+ cells that are Ki67+ (A), CD44+ (B), CD62L- (C) IFN $\gamma$  + (D) or IL-17+ (E) are shown in the top panel; frequencies of CD4+ cells that are Ki67+ (F), Tbet+ (G), IFN $\gamma$ + (H), IL-17+ (I), CD44+ (J), and CD62L- (K) are shown in the bottom panel. The average value for the indicated phenotype of each CC RIX line (n=3) is plotted in black in ascending order on the x axis. B6(red) and BALB/c (blue) baseline values are plotted for comparison. All values represent uninfected controls.

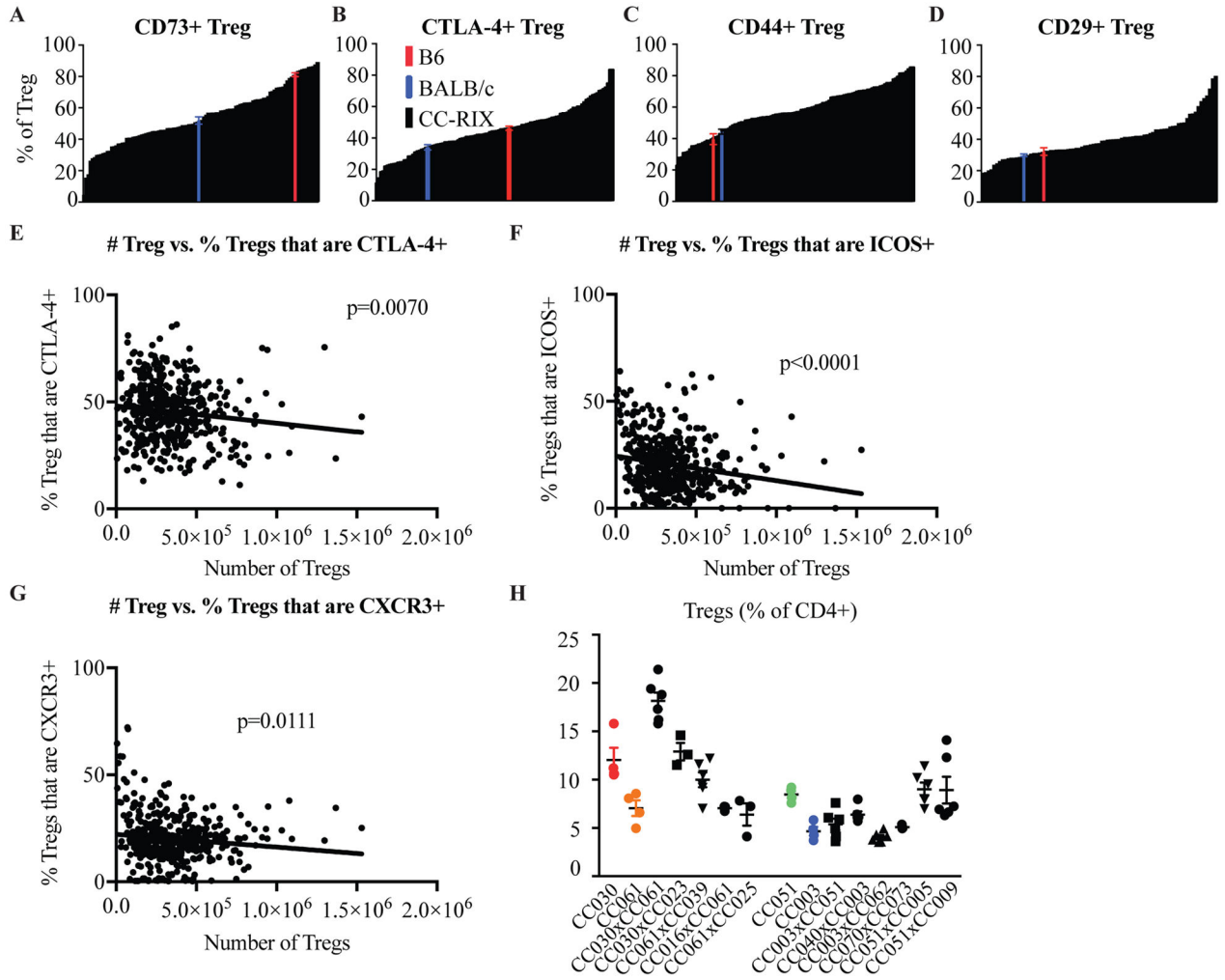


**Figure 3. Differential Treg activation across CC-RIX lines**

Frequencies of Tregs that are CD73+ (A), CTLA-4+ (B), CD44+ (C) and CD29+ (D) across CC-RIX at steady state. The average value for the indicated phenotype of each CC RIX line (n=3) is plotted in black in ascending order on the x axis. B6 (red) and BALB/c (blue) baseline values are plotted for comparison. All values represent uninfected controls. Correlation between the number of Tregs and the frequency of Tregs expressing CTLA-4 (E), CXCR3 (F), or ICOS (G). (H) Comparison of CC-RI lines (colored data points) that served as dams or sires in matings that resulted in RIX lines at the extreme ends of Treg frequency see in figure 2D (black data points).

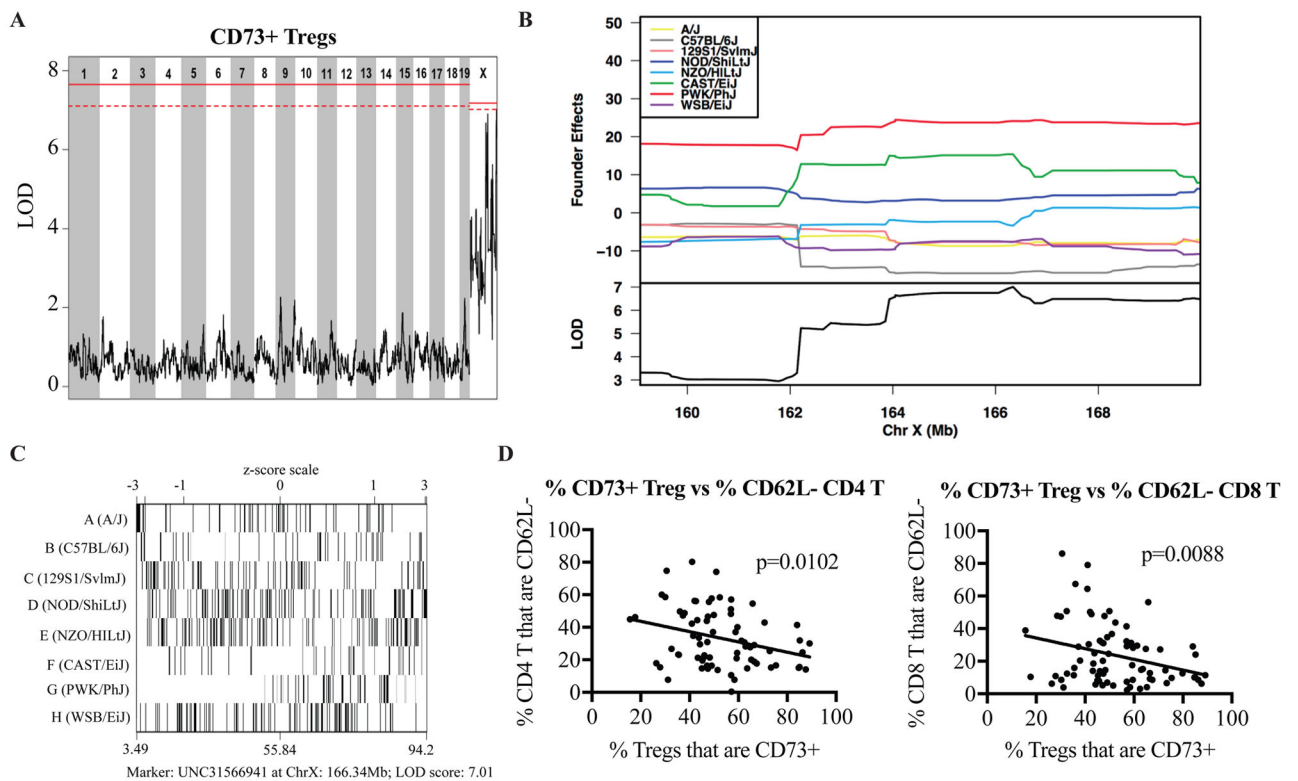


**Figure 4. Quantitative trait loci mapping using the CC**

(A) A QTL driving the frequency of CD73+ Tregs found within the X-chromosome near position 160MB-teomere that appears to be driven largely by a PWK/PhJ founder effect (B). (C) With the frequency of CD73+ Tregs on the x-axis, we see that CC-RIX lines with PWK/PhJ variants at position 166Mb of the X-chromosome have CD73+Treg frequencies at the upper end of the range observed across all CC-RIX examined. (D) Implications on host immunoregulation at the basal state, as there is an inverse correlation between CD73+ Treg frequency and the frequency of activated CD8 or CD4 T cells. In a), the solid red line is the LOD score threshold for  $p=0.05$ , and the dashed line indicates  $p=0.01$ .

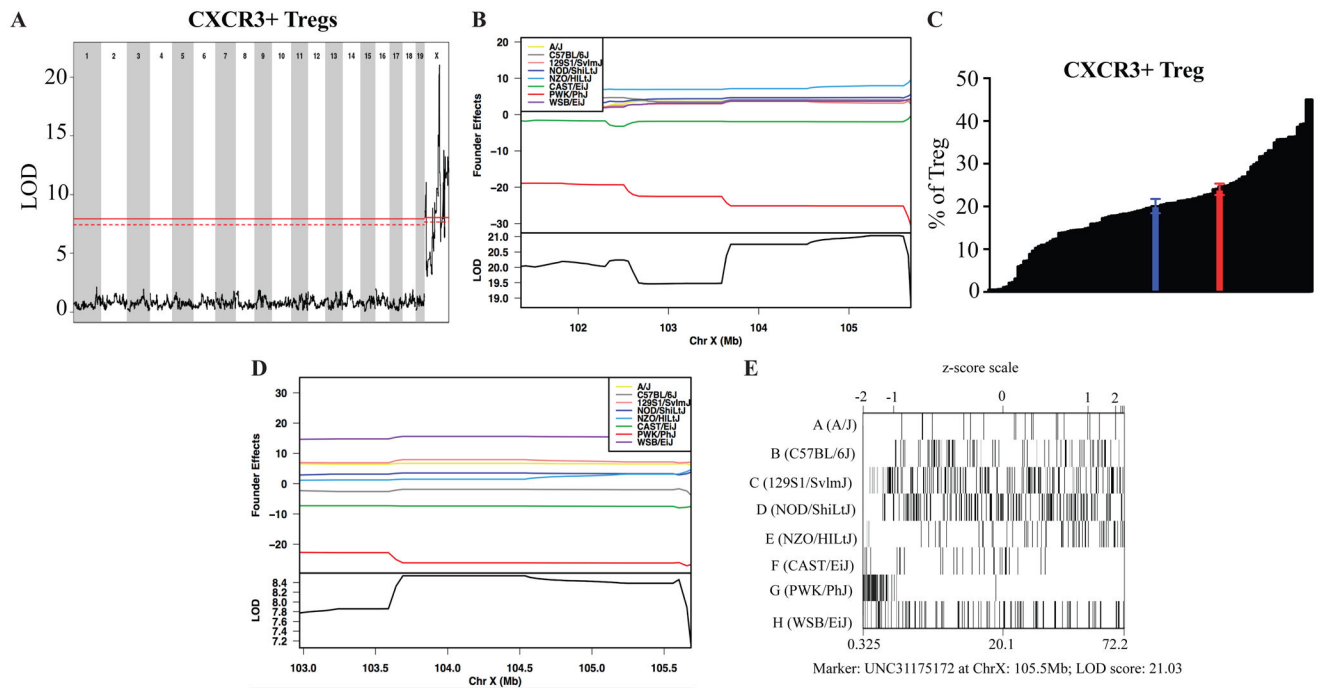


**Figure 5. A highly significant QTL within the X-chromosome drives the frequency of CXCR3+ Tregs**

A QTL was identified within the X-chromosome at position 100–106 Mb (A), driven by PWK/PhJ (B) in all cases with a trend towards lower levels of CXCR3 expression on T cell subsets of CC-RIX lines with PWK/PhJ variants at position 105.5 Mb on the X-chromosome (C, D). Phenotypic-specific allele effects lead to increases in a single phenotype, as there is an NZO/HILtJ effect associated with increased frequency of CXCR3+ Tregs (B) and a WSB/EiJ effect associated with increased frequency of CXCR3+ CD8+ T cells (E). In (A), the solid red line is the LOD score threshold for  $p=0.05$ , and the dashed line indicates  $p=0.01$ .

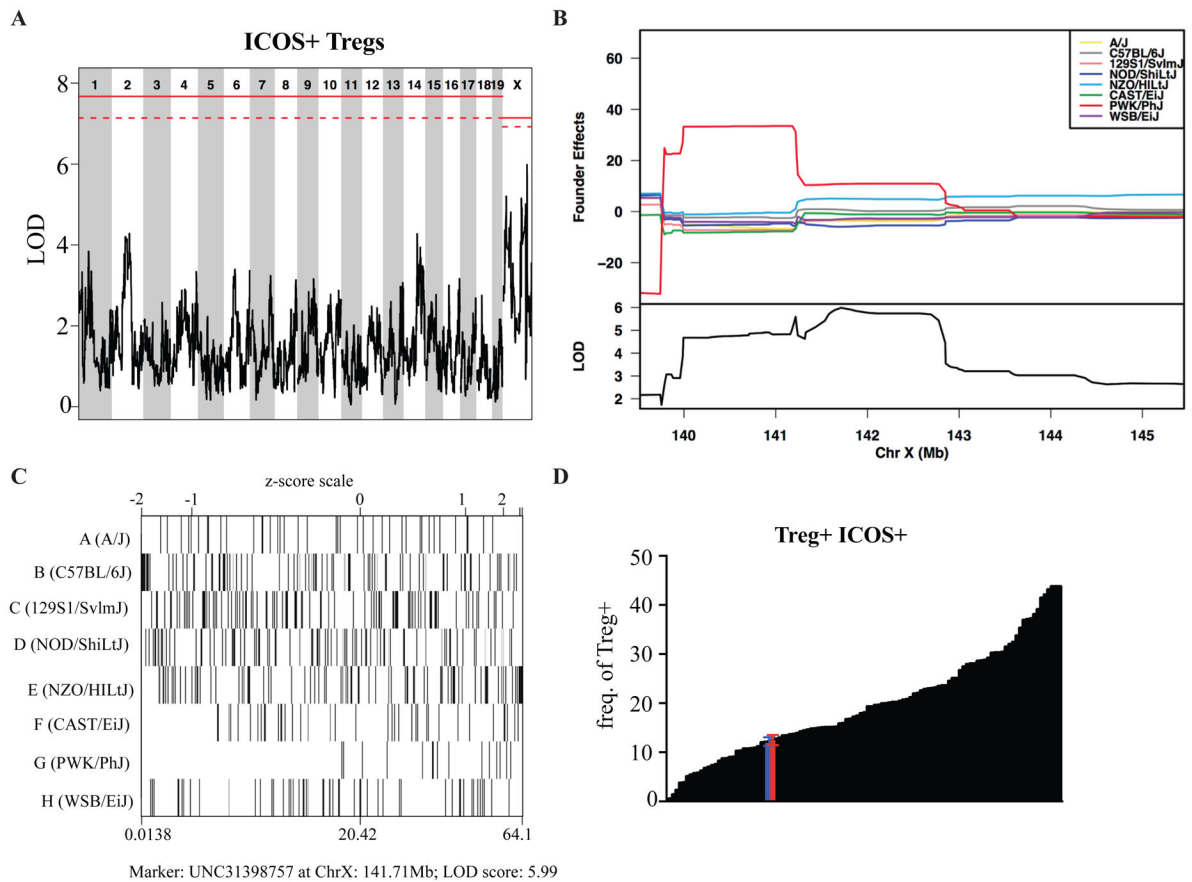


**Figure 6. A QTL driving the frequency of ICOS+ Tregs in the spleen**

A third QTL within the X-chromosome at position 140–145 Mb drives the frequency of ICOS+ Tregs in the spleen (A). An examination of founder effects revealed that the PWK/PhJ allele at position 141.71 Mb drives a high frequency of ICOS+ Tregs (B–C), thereby accounting for the extreme frequency at the higher ranges (D). In (A), the solid red line is the LOD score threshold for  $p=0.05$ , and the dashed line indicates  $p=0.01$ .



**Table 1**

Candidate genes driving select phenotypes of interest.

Phenotype	QTL Region	Founder Effects	Candidate Genes in Region
Frequency of CD73+ Tregs	ChrX: 160 Mb-telomere	PWK high	<i>Arhgap6, Asb11, Ctps2, Egfl6, Figf, Frmpd4, Gemin8, Gja6, Gp464, Map3k15, Mospd2, Nhs, Otd1, Phka2, Piga, Repts2, Rnf138rt1, Syap1, Tceanc, Tlr7, Tlr8, Zsr2, Zrsr2</i>
Frequency of CXCR3+Tregs	ChrX: 100–106 Mb	PWK low	<i>1700011 M02Rik, 8030474 K03Rik, Abcb7, Atrx, Awat1, C77370, Cxcr3, Dgat2l6, Dmrtc1b, Gm5166, Gm9112, Itgb1bp2, Kif4, Magee1, Otud6a, Phka1, Rps4x, Taf1, 170031F 05Rik, Zrsr2</i>
	NZO high		<i>Nhsl2, Kif4, Rgag4, Nhsl2, Asmt</i>
Frequency of ICOS+Tregs	ChrX: 140–145 Mb	PWK high	<i>Ammercr1, Col4a5, Col4a6, E230019M04Rik, Gucy2f, Irs4, Nxt2, Rgag1, Tmem164, Vsig1, Prps1</i>

Author Manuscript

Author Manuscript

Author Manuscript

Author Manuscript